THE AERODYNAMIC DESIGN OF SAILPLANE TAIL ASSEMBLIES

by
Professor E. Eugene Larrabee
Massachusetts Institute of Technology
Cambridge, Massachusetts, U.S.A.

Presented at the XV OSTIV Congress
Rayskala, Finland, 1976

ABSTRACT

The aerodynamic design of a sailplane is dominated by its high aspect ratio unswept wing, which by itself is inherently unstable and uncontrollable in pitch and yaw. A tail assembly of minimum drag and weight must be provided which will permit the pilot to regulate the wing angles of attack and sideslip in normal flight, to overcome towline moments during launch, and to insure recovery from spins. Aerodynamic constraints upon stability and control are examined to determine minimum control surface size, and a simple method, based on biplane theory, is presented for estimation of the vortex drag penalty for tailplane trimming loads. It is concluded that small drag savings can be made with modest weight penalties by adopting longer tail moment arms and higher control surface aspect ratios.

1. Introduction

The design of a sailplane is dominated by the aerodynamic characteristics of its wing. The minimum vortex drag of the wing is given by Munk's well-known formula for elliptic span loading,

$$D_{vortex} \geq \frac{(\text{Lift})^2}{\pi(\frac{\rho}{2}V^2)\ (\text{Span})^2} \qquad (1)$$

but the rest of the drag is due to boundary layer friction and disturbance of the potential flow pressure pattern about the airframe by growth of the boundary layer displacement thickness in the downstream direction. Minimization of the total airframe drag requires airfoil sections and fuselage shapes that will tend to promote laminar boundary layers and that will minimize the skin area in contact with the external flow, at the same time avoiding separation. These requirements have led to the development of very high aspect ratio unswept wings which, by themselves, are not only unstable, but also uncontrollable in pitch and yaw. For this reason it is necessary to provide a tail assembly aft of the wing which will provide adequate levels of stability and control with minimum additional drag and weight.

This paper examines some critical flight situations to determine minimum acceptable tail surface sizes and considers tail geometries which tend to reduce drag and improve stability. It will be shown that lateral control in circling flight tends to establish the vertical tail moment arm, and that the trim drag penalties for a downloaded horizontal tail with the same moment arm as the vertical tail are so small as to make alternative solutions, e.g., sweptback "flying" wings with elevons,* or forward canard surfaces, seem unattractive by comparison.

2. Trim Drag Calculation Using Munk's Stagger Theorem

Let us begin by attacking the "canard" that trimming with an uploaded foreplane is inherently better, an intuitive idea of the Wright brothers which even they abandoned in 1911. We do so by considering the wing-tailplane (or wing-foreplane) combination to be a heavily staggered biplane of very small gap, and calculate its drag with the help of Munk's Stagger Theorem, Fig. 1 (Ref. 1), which states that the induced drag of a multiplane is unaffected by the longitudinal position of its lifting elements so long as the element/element lift ratios and gap/span ratios are preserved. Prandtl (Ref. 2) saw that this would permit the minimum vortex drag of a biplane to be written in the form

---

*See Appendix A for an estimate of the induced drag component of the trim drag for a "flying" wing.

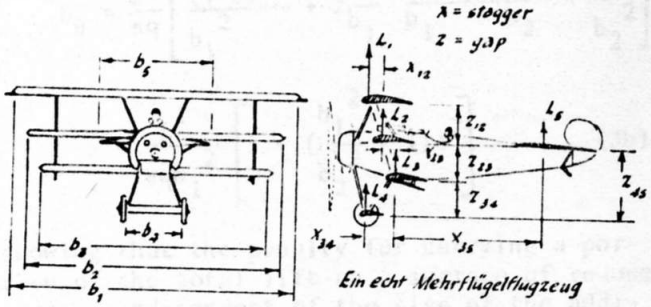

The induced drag of a multiplane is unaffected by the stagger of its individual elements so long as the element/element lift ratios and gap/span ratios are specified.

FIG. 1 MUNK'S STAGGER THEOREM

$$D_{vortex} \geq \frac{1}{\pi q}\left[\frac{L_1^2}{b_1^2} + 2\sigma\,\frac{L_1}{b_1}\,\frac{L_2}{b_2} + \frac{L_2^2}{b_2^2}\right] \qquad (2)$$

where L_1 and b_1 are the lift and span of element (1), L_2 and b_2 are the lift and span of element (2), and $q = 1/2\ \rho V^2$. L_2^2/b_2^2 is proportional to the self-induced drag of element (2), and $2\sigma(L_1/b_1)(L_2/b_2)$ is the cross induced drag of element (1) due to the flow about element (2) plus the cross induced drag of element (2) due to the flow about element (1). Prandtl set Pohlhausen the task of calculating the interference coefficient, σ, for the case of an unstaggered biplane with arbitrary span ratios and gap to average span ratios, assuming that both elements are elliptically loaded, and that the downwash at one element is appropriate to elliptic loading on the other. For an unstaggered biplane the cross induced drags of the two elements are equal, hence the factor 2 in the formula; but for a staggered biplane the *total* cross induced drag is unchanged, that of the forward element being reduced by the upwash ahead of the aft element, and that of the aft element being increased an equal amount by the downwash behind the forward element.

Pohlhausen's values of σ are presented in Fig. 2. It should be noted that σ becomes equal to b_2/b_1 for $b_2 < b_1$ as the gap approaches zero, corresponding to the aft wing being close to the wake of the forward wing, as might be the case for a wing-tail, or a foreplane-wing combination. Fig. 3 presents a comparison of the minimum vortex drag of two wing-trimming plane combinations,

A. a downloaded trimming surface for which

$$L_1 = L\,(1 + \epsilon),\ L_2 = -\epsilon L,\ \sigma = b_2/b_1$$

B. an uploaded trimming surface for which

$$L_1 = L\,(1 - \delta),\ L_2 = +\delta L,\ \sigma = b_2/b_1$$

Substitution into Eq. 2 yields the identical results

$$D_A = \frac{L^2}{\pi q}\left[\frac{(1+\epsilon)^2}{b_1^2} + 2\,\frac{b_2}{b_1}\,\frac{(1+\epsilon)}{b_1}\,\frac{(-\epsilon)}{b_2} + \frac{(-\epsilon)^2}{b_2^2}\right]$$

$$= \frac{L^2}{\pi q b_1^2}\left[1 + \left(\frac{b_1^2}{b_2^2} - 1\right)\epsilon^2\right] \qquad (3a)$$

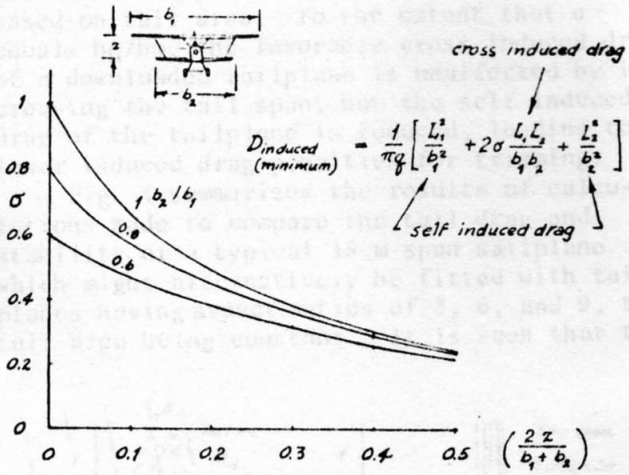

FIG. 2 PRANDTL-POHLHAUSEN BIPLANE INDUCED DRAG FORMULA

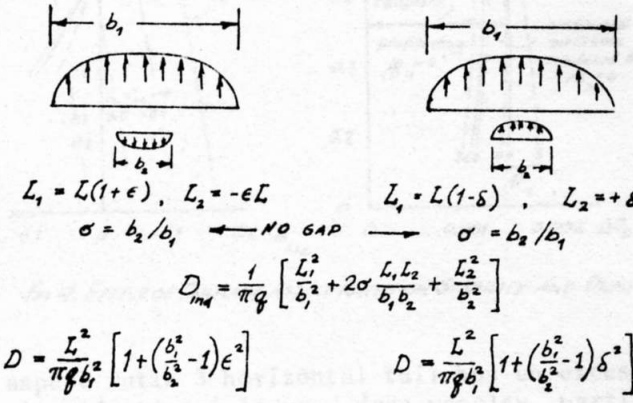

FIG. 3 INDUCED DRAG PENALTY FOR TRIM WITH DOWNLOAD OR UPLOAD

$$D_B = \frac{L^2}{\pi q}\left[\frac{(1-\delta)^2}{b_1^2} + 2\frac{b_2}{b_1}\,\frac{(1-\delta)\,(\delta)}{b_1} + \frac{\delta^2}{b_2^2}\right]$$

$$= \frac{L^2}{\pi q b_1^2}\left[1 + \left(\frac{b_1^2}{b_2^2} - 1\right)\delta^2\right] \qquad (3b)$$

showing that the penalty for carrying a portion of the total lift on a surface of reduced span is independent of the sign of the additional load for a "biplane" of zero gap, a result related to Glauert's harmonic analysis of the lifting line problem in which the total lift is entirely due to the first harmonic, but all harmonics contribute to the vortex drag.

A study of Eqs. 3a and 3b shows that to receive the full favorable effect of the negative cross-induced drag of an uploaded wing-downloaded tail combination, it is necessary for the effective gap to approach zero; on the other hand, the unfavorable effect of the positive cross induced drag of an uploaded wing-uploaded foreplane (or tailplane) combination can be reduced by increasing the gap to average span ratio. Two recent digital computer based finite element models of aircraft aerodynamics have confirmed these ideas: Goldhammer (Ref. 3) has indirectly verified Pohlhausen's values of σ by calculating the reduction of induced drag with increasing gap on an unstaggered biplane having identical wings of elliptic planform, and Tulinius (Ref. 4) has calculated the reduction in trim drag for a canard airframe due to increasing the foreplane span and the vertical spacing between the foreplane and wing surfaces.*

Eq. 2 can be rewritten in a form suitable for calculating the minimum induced drag of a wing-tailplane combination

$$C_{D_{\substack{\text{Vortex}\\\text{Minimum}}}} = \frac{C_{L_W}^2}{\pi(b_W^2/S_W)} + \frac{S_H}{S_W}\left[\frac{2\sigma}{\pi}\,\frac{C_{L_W}C_{L_H}}{b_W b_H/S_W} + \frac{C_{L_H}^2}{\pi(b_H^2/S_H)}\right]$$

where the quantities in the square braces are seen to correspond to tail drag coefficients based on tail area. To the extent that σ equals b_H/b_W, the favorable cross induced drag of a downloaded tailplane is unaffected by increasing the tail span, but the self induced drag of the tailplane is reduced, leading to lower induced drag penalties for trimming.

Fig. 4 summarizes the results of calculations made to compare the tail drag and stability of a typical 15 m span sailplane which might alternatively be fitted with tailplanes having aspect ratios of 3, 6, and 9, the tail area being constant. It is seen that the

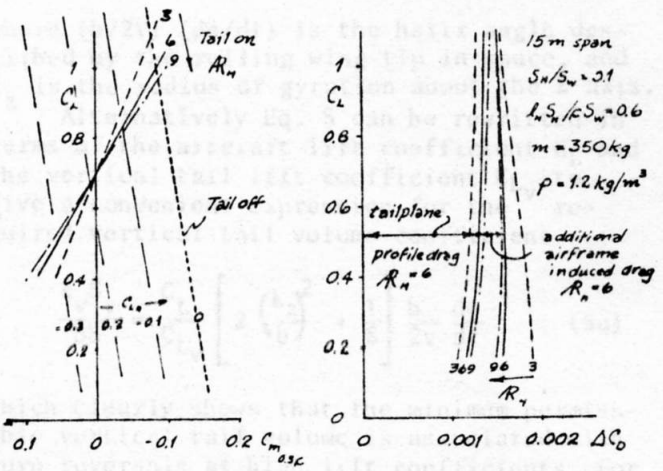

FIG 4. EFFECT OF TAILPLANE ASPECT RATIO ON STABILITY AND DRAG

aspect ratio 3 horizontal tail has an excessive additional induced drag penalty, particularly at low aircraft lift coefficients where appreciable tail load must be carried for trim. All tailplane aspect ratios give about the same drag at high airframe lift coefficients where the tail load is smaller, but the reduced induced drag of the high aspect ratio tails tends to be offset by the unfavorable effect of the tailplane chord Reynolds number which acts to increase the profile drag.

At constant tail volume the high tailplane aspect ratios give a notable increase in static stability, which tends to offset the loss of perceptible aerodynamic control forces with narrow chord tailplanes. The as-

*After this paper was given at NASA Langley, McLaughlin (NASA Technical Note D-8391, May 1977) made a comprehensive study of trim drag for canard and conventional airframes by the method discussed here which showed the superiority of the downloaded aft tail with various practical constraints and also showed good agreement with Tullinus' elaborate vortex lattice theory.

pect ratio 9 tailplane, for example, would have a chord of only 333 mm for a span of 3 m, and might well be constructed like a section of helicopter rotor blade, pivoted about its quarter chord and mass balanced throughout its length. Such a tailplane would undoubtedly require a centering spring which might be biased for longitudinal force trim together with a control linkage bobweight to insure "g" feel.

To sum up this study of tail drag including the effects of trim drag, it would appear that the additional drag of downloaded aft tailplanes of normal size is rather small, amounting to something like 20-30% of the profile drag of the wing. There is no real advantage in trimming with an upload. Some small gains are available at high speeds and low lift coefficients for downloaded tailplanes of high aspect ratio mounted low so as to be close to the wing wake at low and moderate angles of attack, i.e., a high wing, low tail configuration.

3. Vertical Tail Loads in Turn Reversals

As a general rule, the tail moment arm of a sailplane is set by lateral stability and control considerations. One of these, which is simple to calculate, is the vertical tail load needed to reverse a coordinated turn, Fig. 5 (Refs. 5 and 6). Since the aircraft Z axis component of the rate of turn is proportional to the sine of the roll angle, it follows that during a turn reversal a yawing acceleration must be imparted to the aircraft which is proportional to the product of the cosine of the roll angle and the roll rate. As the aircraft rolls through wings level at constant angular velocity, the lift vectors are rotated forward on the down going wing and aft on the upgoing wing through the local helix angle, giving rise to an adverse yawing moment due to rolling (which is indistinguishable from aileron drag). Assuming that the sum of the adverse yawing moments due to rolling and aileron drag is given by resolving a distorted elliptic lift distribution onto the XY plane, it follows that the tail load required for turn reversal is given by

$$-\frac{Y_v}{mg} = \frac{b}{\ell_v}\left[2\left(\frac{k_z^2}{b^2}\right) + \frac{1}{8}\right]\left[\frac{b}{2V}\frac{d\phi}{dt}\right] \qquad (5)$$

where $(b/2V)(d\phi/dt)$ is the helix angle described by the rolling wing tip in space, and k_z is the radius of gyration about the Z axis.

Alternatively Eq. 5 can be rewritten in terms of the aircraft lift coefficient C_L and the vertical tail lift coefficient C_{L_v} to give a convenient expression for the required vertical tail volume coefficient

$$\frac{\ell_v S_v}{bS} = \frac{C_L}{C_{L_v}}\left[2\left(\frac{k_z}{b}\right)^2 + \frac{1}{8}\right]\frac{b}{2v}\frac{d\phi}{dt} \qquad (5a)$$

which clearly shows that the minimum permissible vertical tail volume is associated with turn reversals at high lift coefficients. For example, if full aileron deflection will maintain a helix angle of 0.1 radian, $k_z = b/4$, and $C_L/C_{L_v} = 1.4/1.2$

$$\frac{\ell_v S_v}{bS} = \frac{1.4}{1.2}\left[2\left(\frac{1}{4}\right)^2 + \frac{1}{8}\right](0.1) = 0.02917$$

and for $l_v/b = 4/15$, $S_v/S = 0.10917$ Eq. 5 reassures us that if the tail structure is large enough and strong enough to perform a coordinated turn reversal at minimum speed, it is also strong enough to perform a turn reversal at high speed since the aircraft will always roll at the same helix angle if the ailerons can be fully deflected.

It is clearly desirable to increase the vertical tail arm on the basis of this analysis since the same yawing moment tends to be required independent of the tail length, the inertia in yaw being dominated by the wing contribution, and the adverse aerodynamic yaw being entirely due to the wing. A longer tail arm allows the vertical tail size to be reduced with benefits in surface weight and drag. From the structural standpoint it would be desirable to connect the vertical tail boom directly to the wing structure since this re-

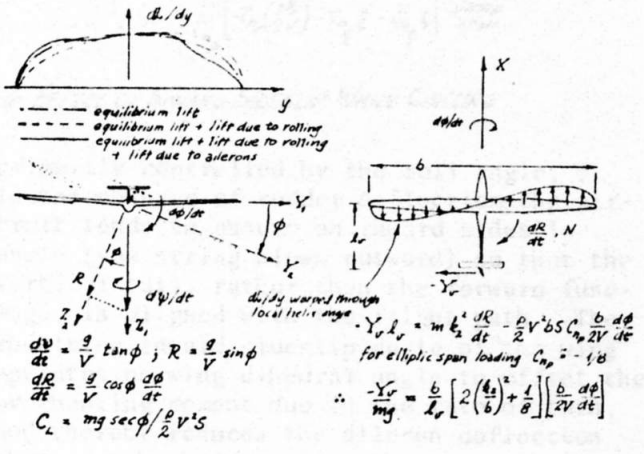

Fig. 5 Vertical Tail Loads During a Turn Reversal

duces the length of the load path. A long vertical tail arm also favors spin recovery, and promotes resistance to spin entry. My teacher, Professor Koppen, always maintained that a vertical tail arm equal to the wing semispan was essential for satisfactory lateral control of propeller driven airplanes, a rule which no current sailplane meets.

4. Drag in Circling Flight

Another reason for a longer vertical tail arm lies in the inherent tendency toward inward sideslip angle during circling flight, Fig. 6. The rate of turn, Ω, is

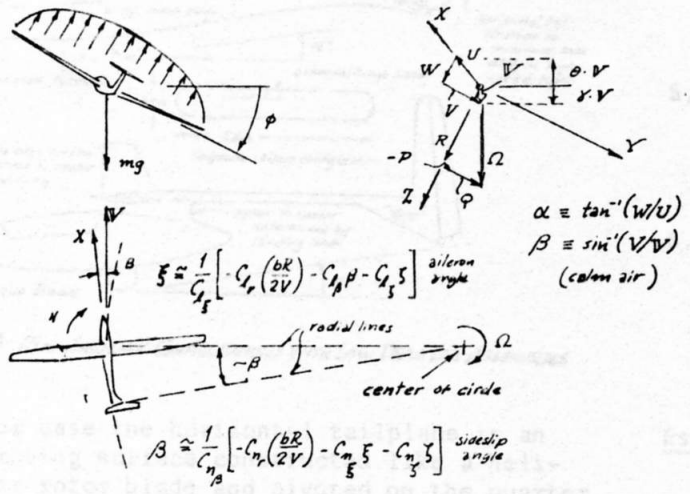

FIG. 6 EFFECT OF INWARD SIDESLIP WHILE CIRCLING

primarily controlled by the roll angle, ϕ. In the absence of rudder deflection the aircraft tends to assume an inward sideslip angle (yaw string blown outward) so that the vertical tail, rather than the forward fuselage, is aligned with the flight path. The resulting inward sideslip angle of the wing operates on wing dihedral angle to offset the overbanking moment due to the rate of turn, and thereby reduces the aileron deflection that must be held against the turn. At the same time the sideslip of the wing-body combination tends to produce outward sideforce and a certain amount of vortex drag. For every sailplane there is an optimum sideslip angle that ought to be held during circling flight which is a function of roll angle, dihedral angle, and drag penalties for aileron deflection, rudder deflection, and vortex drag due to sideforce. Drag due to rudder deflection and sideslip is reduced by increasing the depth of the fuselage. The author has estimated the circling drag of a hypothetical sailplane as a function of sideslip angle for one roll angle in Ref. 5. The drag contributions are plotted as a function of sideslip angle in Fig. 7.

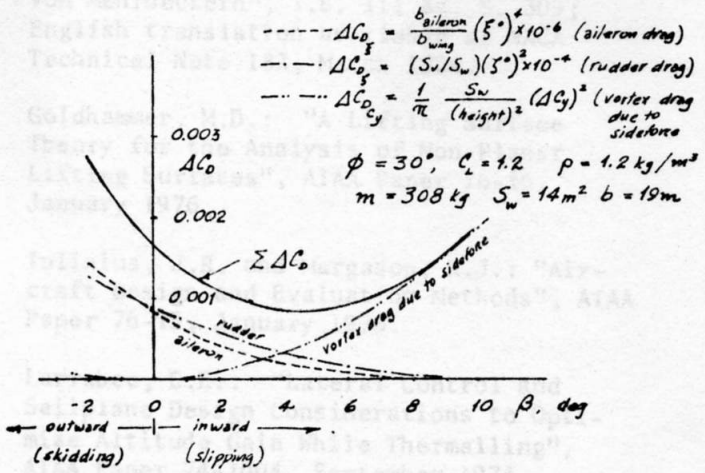

FIG. 7 EFFECT OF SIDESLIP ON CIRCLING DRAG

5. Tail Design for Minimum Drag and Other Considerations

A brief examination of tail drag penalties has shown that increasing tail surface aspect ratio is desirable because of reduced trim drag penalties, both in pitch and yaw. A vertical tail volume requirement is more apt to be critical than a horizontal tail volume requirement because of a simple need to overcome the large inertia of the wing in yaw during turn reversals, and the absence of a similar requirement for pitching maneuvers. Inappropriately located tow hooks may very well determine the horizontal tail volume requirement, but this situation can always be improved in principle by location of the hook so that the extended towline axis passes through the center of gravity.*

Somewhat longer tail arms appear to be desirable, particularly from the standpoint of lateral control and drag during circling flight. Longer tail moment arms have reduced torsional rigidity for a given bending strength and raise the possibility of flutter, particularly for T tail configurations. V tail configurations are perhaps more acceptable from the flutter standpoint, but they

*Appendix B describes the dynamics of a typical winch launch and provides some typical values for towline loads.

probably should be constructed with dihedral angles of less than 90° between their upper surfaces to improve the yawing moment capability. Both T tails and V tails (but not inverted V tails) lead to larger induced drag penalties in high speed flight for the typical case of tailplane download for trim. The principal justification for T tails and V tails would appear to be minimization of tail surface damage in off airport landings.

Fig. 8, finally, shows a pair of tail assemblies appropriate to 15 m sailplanes. In

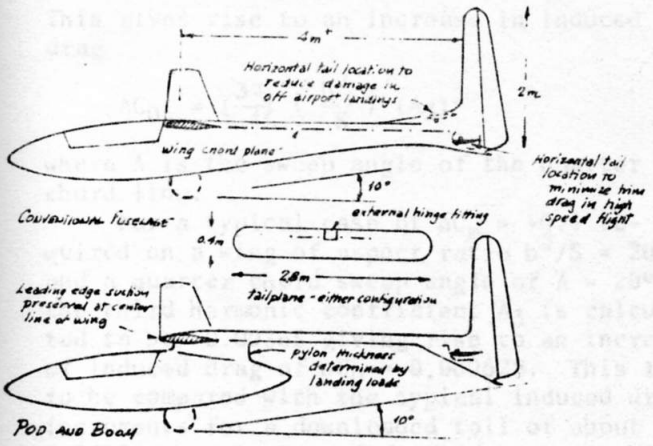

FIG. 8 15m SAILPLANE CONFIGURATIONS WITH LOW DRAG TAIL ASSEMBLIES

either case the horizontal tailplane is an all moving surface constructed like a helicopter rotor blade and pivoted on the quarter chord line with a hinge fitting external to the surface. Control feel and force trim is provided by springs. The horizontal tail should be cambered to favor downloads.

The vertical tail has a symmetrical section with a 45% chord rudder. It would be desirable to center its area on the torsional axis of the aft airframe structure, an arrangement which leads to the pod and boom configuration shown. In the pod and boom configuration, the boom is attached with structural bolts to the rectangular center section of a three piece wing, and the pod is separately bolted to the wing-tail boom assembly. The pod pylon is mainly designed to take landing gear sideloads, and might be bolted to the wing-tail boom assembly with bolts of limited lateral strength. The pylon mounting permits the development of unbroken leading edge suction at high lift coefficients, thereby improving the maximum lift coefficient and reducing airframe drag at the lift coefficients for minimum sinking speeds.

REFERENCES

1. Munk, M.: "Isoperimetrische Aufgaben Aus der Theorie des Fluges" dissertation, Goettingen 1919.

2. Prandtl, L.: "Der Induzierte Widerstand von Mehrdeckern", T.B. III Bd. S. 309; English translation available as NACA Technical Note 182, March 1924.

3. Goldhammer, M.D.: "A Lifting Surface Theory for the Analysis of Non-Planar Lifting Surfaces", AIAA Paper 76-16, January 1976.

4. Tulinius, J.R. and Margason, R.J.: "Aircraft Design and Evaluation Methods", AIAA Paper 76-15, January 1976.

5. Larrabee, E.E.: "Lateral Control and Sailplane Design Considerations to Optimize Altitude Gain While Thermalling", AIAA Paper 74-1004, September 1974.

6. Larrabee, E.E.: "Vertical Tail Size Needed for a Coordinated Turn Reversal, AIAA *Journal of Aircraft*, Vol. 12, No. 8, pps. 687-688.

APPENDIX A

Estimation of the Trim Drag for a Sweptback "Flying Wing" Airframe

The sweptback "flying" wing airframe is a perennial weed in the garden of applied aerodynamics (c.f., J.K. Northrop's XB-35 and XB-48; also various experimental sailplanes and research airplanes by the Horton brothers in Germany). The absence of a vertical tail capable of providing strong yawing moments on the verge of stall is the principal shortcoming of the type. It also has a trim drag penalty with an easily calculated induced drag component.

The additional lift due to an increase in angle of attack may be assumed to be approximately elliptic and to be centered longitudinally on the local quarter chord lines; the center of gravity location must be slightly behind a line joining the centroids of the half elliptic lift distributions on the port and starboard wing halves at 42.4% of the semi span for $\partial C_m/\partial \alpha$ to be negative. Now assume a combination of wing twist and/or elevon deflection giving rise to the third harmonic of a Glauert Fourier series lift distribution as shown in the figure, which

can be used to trim wing section pitching moments and lift at high angles of attack. The third harmonic lift distribution produces an aerodynamic moment on each wing half perpendicular to the quarter chord line which can be resolved into components parallel (M_X) and perpendicular (M_Y) to the direction of flight. In this way a relation is found between the pitching moment and the size of the third harmonic:

$$\Delta C_m = (\tan \Lambda)\left(\frac{b^2}{S}\right)^2(-0.188225\ A_3)$$

This gives rise to an increase in induced drag

$$\Delta C_{D_i} = \left(\frac{3\pi}{4}\right)\left(\frac{b^2}{S}\right)(A_3)^2$$

where Λ is the sweep angle of the quarter chord line.

For a typical case of $\Delta C_m = +0.1$ required on a wing of aspect ratio $b^2/S = 20$ and a quarter chord sweep angle of $\Lambda = 20^\circ$, the third harmonic coefficient A_3 is calculated to be -0.00365 giving rise to an increase of induced drag of $\Delta C_D = 0.000628$. This is to be compared with the typical induced drag increments for a downloaded tail of about 0.0003 shown in Fig. 4 for the same pitching moment coefficient.

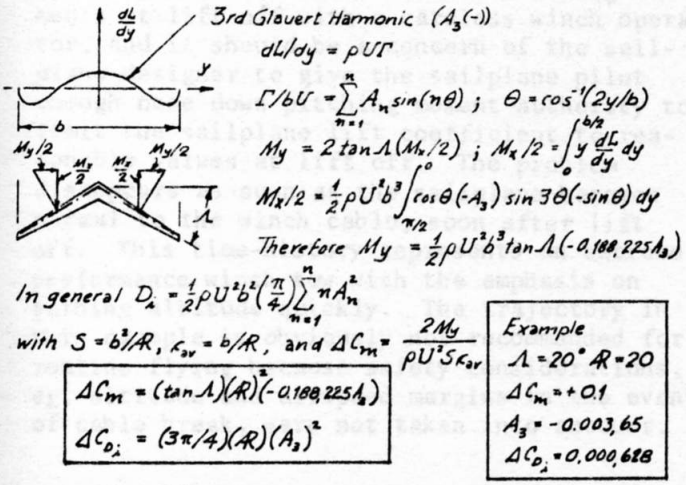

Induced Drag Penalty for Trimming with Twist and Sweep

APPENDIX B

Towline Loads in Winch Launches

In a winch launch the sailplane is pulled into the air by a cable reeled onto a drum. The launch process is under mutual control of the glider pilot, who can regulate the sailplane angle of attack and lift coefficient by means of elevator deflection, and the winch operator, who can control the cable tension by regulating the winch speed. The cable tension is limited by a length of reduced tensile strength cable near the sailplane, and by the power-speed characteristics of the winch engine-transmission combination. These relations are summarized in Fig. 1.

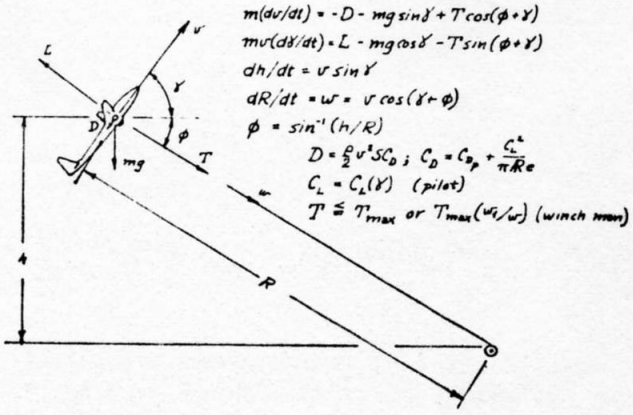

(1) *Mathematical Model of the Winch Launch Process*

Vlado Lenoch, in his M.I.T. Masters Thesis, *An Aerodynamic Study of Horizontal Tailplane Configurations and Sizing*, (Sept. 1976) programmed these equations for numerical integration on a small digital computer and obtained many representative solutions, one of which is given in Fig. 2.

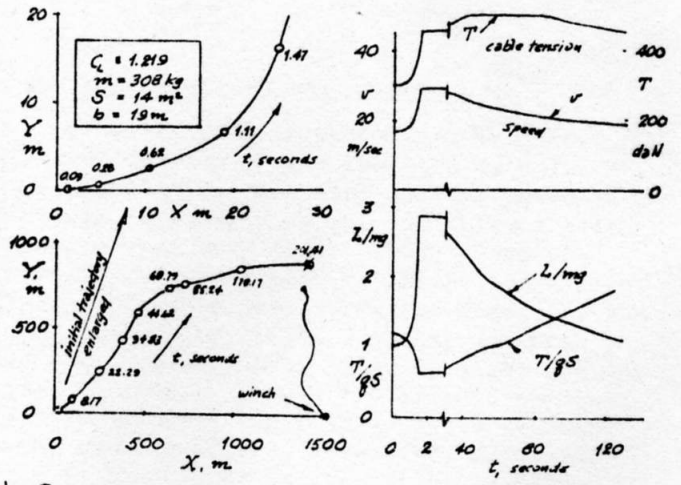

(2) *Representative Winch Launch Process*

In this launch the pilot is assumed to hold the sailplane trimmed at maximum lift coefficient. The sailplane accelerates rapidly and pulls up at a steep angle. After 1.47 seconds the flight path is almost perpendicular to the cable, and the winch operator must slow the winch appreciably to limit the wing lift load to 2.9 times the sailplane weight. Thereafter modest winch speeds keep the sailplane rising like a kite with appreciable line tension. From 40 to 80 seconds into the launch the cable tension approaches its limit value of 600 daN (approximately 600 Kg "force"). As the trajectory rounds over the sailplane is allowed to decelerate to its stalling speed in level flight and finally the pilot releases the line after 200 seconds, practically over the winch.

The ratio of cable tension to dynamic pressure times wing area, T/qS has large values both at the beginning of the launch and at the end. The trimming lift coefficient that has to be supplied by the tail is proportional to T/qS and the ratio of the tow hook arm about the center of gravity to the tail volume, $\frac{\text{hook arm}}{l_H S_H}$. A common compromise is to place the hook on the landing gear support structure where it is near the center of gravity longitudinally but not vertically. This may lead to uncontrollable stalling moments at lift off with a careless winch operator, and it should be a concern of the sailplane designer to give the sailplane pilot enough nose down pitching moment authority to limit the sailplane lift coefficient to reasonable values at lift off. The problem disappears as soon as the sailplane becomes normal to the winch cable, soon after lift off. This time-history represents an extreme performance winch tow with the emphasis on gaining altitude quickly. The trajectory in this example is obviously not recommended for routine flying because safety considerations, eg, altitude and airspeed margins in the event of cable break, were not taken into account.